ELECTRONIC SAR PROCESSORS FOR SPACE MISSIONS*

CHIALIN WU
JET PROPULSION LABORATORY
CALIFORNIA INSTITUTE OF TECHNOLOGY
PASADENA, CALIFORNIA 91103

SUMMARY

This paper reports some interim results relating to an on-going effort to develop an electronic processor for real-time processing of synthetic aperture radar data. An experimental laboratory processor is being developed as a testbed for design of on-board processors for future space missions. This paper describes the configuration of the experimental processor and discusses technical factors pertaining to the design.

1.0 INTRODUCTION

The utility of airborne synthetic aperture radar (SAR) [1] [2] has been extensively investigated in the past two decades. Because of the capability of microwaves to penetrate through clouds and the unique contrast characteristics in SAR imagery, radar imaging is considered particularly useful for· surface topographic mapping and for all-weather sea state observations. To extend the utility of airborne SAR so that the imaging radar could also be used as a global environmental monitoring device, NASA is planning to launch a series of earth and planetary spacecraft with on-board imaging radars. The SEASAT-A satellite which will be launched in May 1978, is the first in the series. The SEASAT-A radar is designed to be able to produce imagery with 25 meter resolution and 100 km swath width on the earth's surface [3].

The high resolution and wide swath coverage called for by the SEASAT-A SAR imply an extremely high data acquisition rate. SEASAT-A will use a newly developed ground-based digital tape recorder with 120M bits per second recording capability. The large amount of SAR data acquired must be processed

---

to produce images in a satisfactory format. Due to various peculiarities in the doppler characteristics of spaceborne SAR data, the SAR processing and associated compensation procedures can be very involved. Currently available SAR processors are not able to produce the imagery in a timely and economic manner.

Although SEASAT-A SAR sets a data acquisition rate from the spaceborne sensor that is unprecedented, future earth orbit imaging radars may adopt similar performance criteria and data acquisition requirements. An effective way to meet the data processing needs in future anticipated operational radar imaging missions is to employ on-board SAR processors. Such on-board processors would produce SAR imagery from echo signals in realtime. Not only can the transmission bandwidth for imagery data be reduced by a large factor (compared with the unprocessed raw data transmission rate), but direct image transmission to users in the vicinity of the sensor also simplifies the data handling and distribution procedures.

To achieve the goal of on-board SAR processing, JPL initiated a phased development task in the beginning of FY 77. The first phase involves develop-ment of a ground based experimental SAR processor. This processor will have the capability to perform realtime SAR processing. The processor architecture and device technology will be chosen to be amenable to future on-board implementation. After its completion, scheduled for the end of FY 79, the performance of the processor will be evaluated by processing a 20 km swath of the then available SEASAT-A SAR data at the real-time data rate. The output image data will comprise 4 looks and exhibit 25M resolution. The next phase of the work involves the design and construction of a SAR processor to be used in an on-board processing experiment on a future Shuttle Imaging Radar (SIR) mission. Also, it is anticipated that a simple low-resolution on-board SAR processor will be developed for a 1983 Venus Orbital Imaging Radar (VOIR) Mission. The development of these two on-board processors may begin prior to the completion of the ground based experimental processor. Nevertheless, concepts, details of the design, and perhaps some specially developed devices will be directly applicable to these follow-on activities. Although the emphasis has been placed on the development of on-board SAR processors, the

ground-based experimental SAR processor naturally will serve also as a model for real-time ground station processing of future spacecraft-gathered SAR data.

The task of developing the experimental SAR processor was divided into the following three phases: the system design, the detailed design, and the implementation. The system design phase was concluded near the end of FY 77. The task is currently in the phase of detailed design. Major issues resolved in the system design phase include the formulation of the design requirements, the selection of the correlator architecture, and the development of real-time processing control procedures. This paper reports some results related to the processor system design and analysis. A brief description of the overall system will be given first. Study results related to the spaceborne SAR doppler characteristics will be discussed to establish the design requirements for the azimuth correlator. Discussion then proceeds to the criteria for selecting a correlator architecture, the clutterlock approach, and the procedures for generating processing parameters in real-time.

2.0 SAR PROCESSOR REQUIREMENTS

An important reason for developing the experimental SAR processor is to obtain a breadboard applicable to several future operational spaceborne SAR missions. To meet this objective, the data processing needs for several anticipated future spacecraft SAR missions were analyzed to establish a set of design requirements and guidelines for the experimental processor. Those anticipated missions include the Shuttle Imaging Radar (SIR) flights, the 1983 Venus Orbital Imaging Radar (VOIR), and the SEASAT follow-up missions. Most of these missions are still in the planning stage. The radar parameters and the performance criteria are not yet fully established. The mission objectives, however, are expected to require a high resolution imaging mode, which provides multiple-look images at a spatial resolution comparable to the 25 meter resolution required by SEASAT-A. This observation in conjunction with the fact that SEASAT-A SAR data will be the only spaceborne SAR data available by the end of 1979 lead to the selection of the SEASAT-A SAR as the reference radar sensor for the development. The sensor characteristics and the performance requirements of the experimental processor (adopted from the SEASAT-A specifications) are tabulated in Table 1. A modular approach was chosen to simplify the problem of processing data over a wide swath. A swath width of 20 km, which is one-fifth of the SEASAT-A SAR swath, was chosen for the experimental SAR processor.

TABLE 1

SENSOR CHARACTERISTICS AND PERFORMANCE REQUIREMENTS

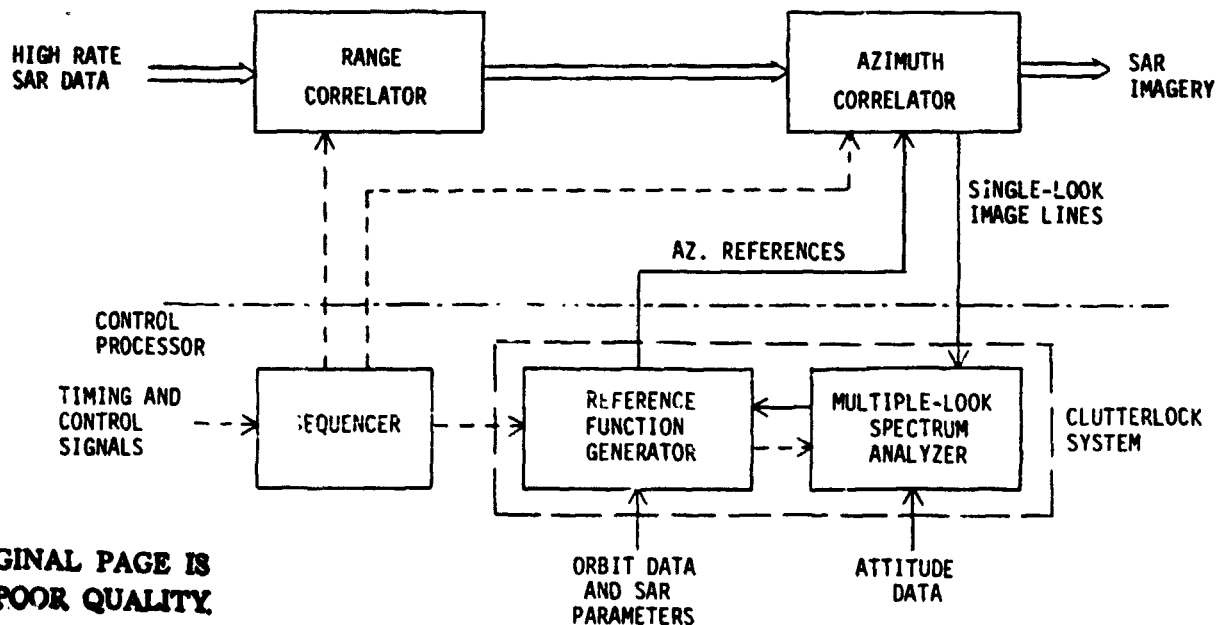OF THE EXPERIMENTAL SAR PROCESSOR

SAR System Parameters (SEASAT-A SAR)

SAR Orbit	SEASAT-A Orbit
Nominal Altitude	794 km
Nominal Speed	7450 m/sec
Transmitter Frequency	1275 MHz
Pulse Repetition Frequency	1463,1537,1645 Hz
Pulse Width	33.8 μ sec
Pulse Bandwidth	19 MHz
A/D Rate for Range Offset Signals	45.03 MHz
A/D Window	288 μ sec
Antenna Dimension	2m X 10.5m
Antenna Look Angle	20° cone, 90° clock
Attitude (roll, pitch, yaw) Accuracy	$\pm0.5^\circ$

Experimental Processor Performance Requirements

Image Swath	20 km
Image Resolution	25 m
Number of Looks	4
Image Dynamic Range	50 dB
Data Processing Speed	Real-Time Rate

3.0 EXPERIMENTAL SAR PROCESSOR CONFIGURATION

A block diagram of the experimental SAR processor is shown in Figure 1. The three major elements in the processor are the range correlator, the azimuth correlator, and the control processor. The range correlator compresses the transmitted pulse waveform into a short pulse. The synthetic aperture processing which refines the antenna azimuth beamwidth is performed in the azimuth correlator. The control processor is mainly responsible for the generation of a target response function which is matched to the received echo signals. The control processor also produces various timing signals to synchronize the data processing operations. The block diagram shown in Figure 1 also indicates that the range correlation is performed prior to the azimuth correlation. This order can not be altered since the azimuth Doppler response of a target is range dependent. A more detailed discussion of this requirement is given in [4].

ORIGINAL PAGE IS
OF POOR QUALITY

Fig. 1 The Experimental SAR Processor Blockdiagram

The design of the data flow rate in the processor also needs some special consideration. It is necessary to accommodate different pulse repetition frequency (PRF) values. The sampling frequency of the received echo is determined by the radar bandwidth, and thus is independent of the PRF. To make the system tolerant of changes in the value of the PRF, a harmonic of the PRF is used to synchronize the data processing operations. In multi-look processing, the image data output from the overlay register occurs in bursts.

Time expansion to achieve a near uniform output rate is desirable. A constant clock rate derived from the input sample clock can be used to produce a uniform output data rate. In this arrangement, the input and ou...... data rates are properly matched and are independent of PRF changes.

The range c elation in SAR processing is a relatively straightforward function compared with the synthetic aperture processing. Also, it is antici-
; ted that future missions will use transmitter codes other than the linear FM chirp of SEASAT-A SAR. For these two reasons, it is planned to utilize programmable digital matched filters for the experimental SAR processor.

The development emphasis is on the synthetic aperture processing. Detailed discussions relating to the azimuth correlator and the control processor are given in the following sections.

4.0 SYNTHETIC APERTURE PROCESSING FOR THE SPACEBORNE RADARS

Accurate knowledge of the target Doppler characteristics is essential to produce high quality spaceborne SAR imagery. The factors which determine the target Doppler characteristics are therefore discussed in detail.

4.1 THE SPACEBORNE SAR DOPPLER CHARACTERISTICS

In a coherent radar system such as a SAR, the variation of phase in the returned signals is directly related to the distance history between the sensor and the target. The analysis of doppler phase history thus is equiv-
alent to the study of the relative motion between the sensor and targets on the planet surface. The relative motion problem for a spaceborne SAR is usually more complex than that for an airborne SAR. For the spaceborne SAR, both the sensor and targets must be treated a. moving bodies. The problem in many cases is further complicated by the fact that the curvature of the planet's surface causes the target velocity vector to depend upon the position of the target in the swath. To analyze the problem, we have assumed an elliptical spacecraft orbit and an oblate planet surface. The position of the spacecraft in the orbit is first chosen according to a specified orbit latitude angle. The position of the target then can be determined by specifying a radar attitude angle. Assuming that $\bar{R}o$, $\bar{V}o$, and $\bar{A}o$ are respectively, the relative position, velocity, and acceleration vectors over a very short period of synthetic aperture integration then the distance history, $R(t)$, can be approximated by the following expression:

$$R(t) \cong |\vec{R}_o| + \left(\frac{\vec{V}_o \cdot \vec{R}_o}{|\vec{R}_o|} \right) t + 1/2 \left(\frac{|\vec{V}_o|^2}{|\vec{R}_o|} + \frac{\vec{A}_o \cdot \vec{R}_o}{|\vec{R}_o|} \right) t^2 \tag{1}$$

With the distance history shown above, the phase history, $\phi(t)$, can be approximated as follows:

$$\phi(t) \cong \phi_o + F \cdot t + 1/2\ \dot{F}\ t^2 \tag{2}$$

where

$$F = \frac{2}{\lambda} \frac{\vec{V}_o \cdot \vec{R}_o}{|\vec{R}_o|} \tag{3}$$

$$\dot{F} = \frac{2}{\lambda} \left(\frac{|\vec{V}_o|^2}{|\vec{R}_o|} + \frac{\vec{A}_o \cdot \vec{R}_o}{|\vec{R}_o|} \right) \tag{4}$$

and λ is the radar wavelength. The two factors F and $\dot{F}$ shown above are the instantaneous doppler frequency and the doppler chirp rate at the center of the aperture. Eqs. 2 and 3, show that the doppler center frequency is a function of relative speed along the radial direction, whereas the doppler chirp rate is a function of the relative acceleration. The first term in the radial acceleration can be referred to as the centrifugal acceleration. The second term is a direct result of the acceleration vector which is mainly due to the gravitation effect on the spacecraft free orbit motion.

A numerical study of the sensor-target relative motion problem showed that Eq. 2 provides an accurate measure of the phase history over the full 2.5 second SAR integration time required by SEASAT-A. This leads to the conclusion that the doppler frequency and the doppler chirp rate are the two most important parameters for azimuth correlation. Assuming a plus and minus one degree variation in the antenna roll, pitch, and yaw altitude, the range of doppler frequencies and chirp rates that the azimuth correlation must accept are plotted in Figures 2 and 3. These two figures show that the doppler frequency and chirp rate are dependent upon both the spacecraft position and the target
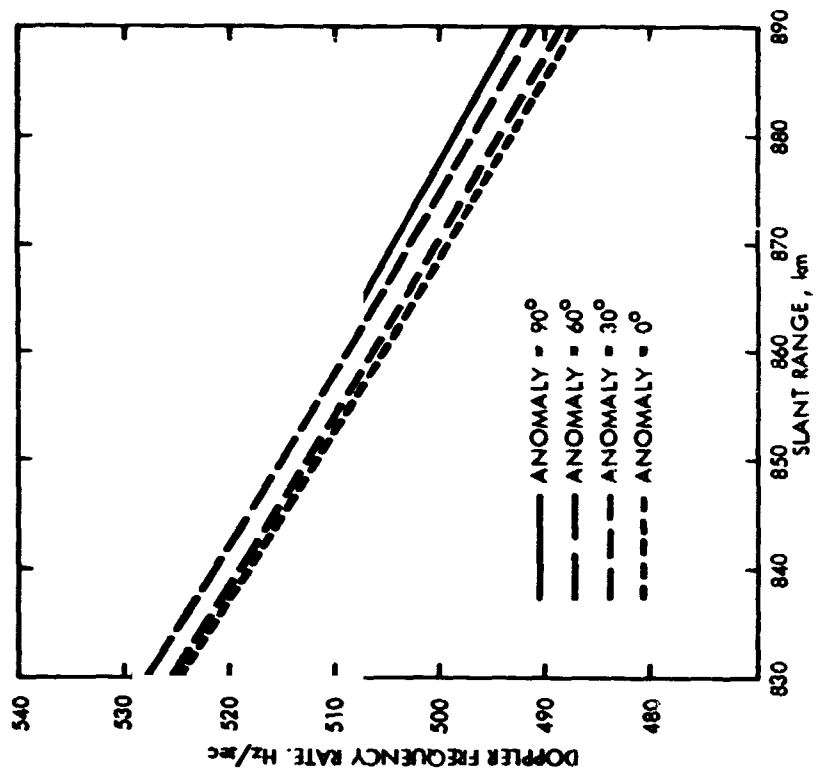
Fig. 3   SEASAT-A SAR Doppler Frequency
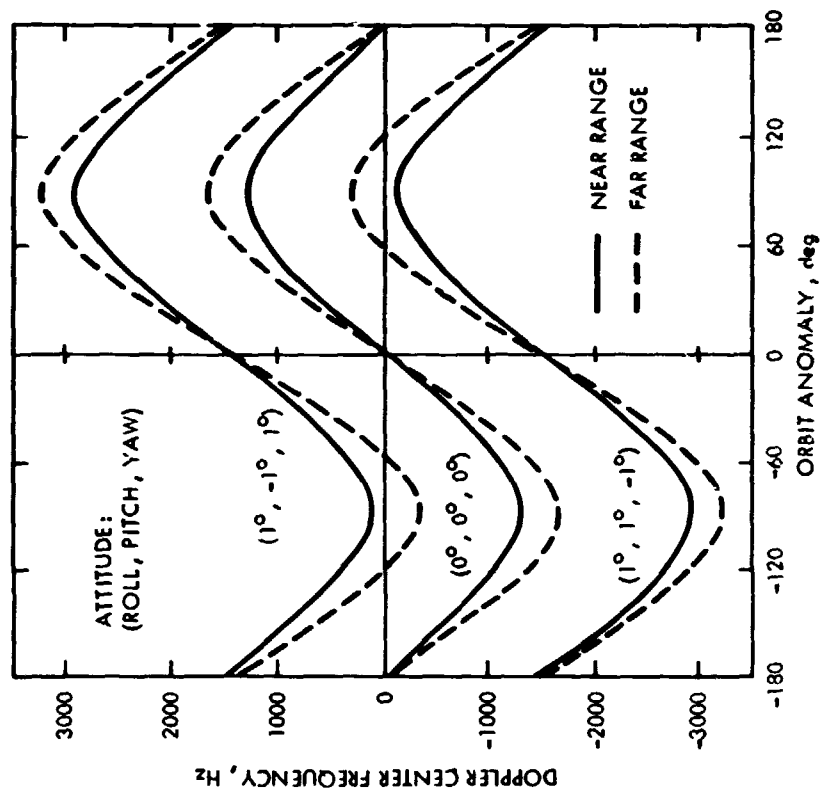Rates at Four Orbit Positions

Fig. 2   SEASAT-A SAR Doppler Frequency
Characteristics

V-3-8

slant range. The azimuth correlator, therefore, must be designed to accommodate such variations in the processing parameters.

Two major design requirements of particular importance are the synthetic aperture integration time and the amount of range migration to be compensated over the aperture width. The required integration time is determined based on the following factors: the doppler chirp rate shown in Figure 2, the sensor speed relative to the planet's surface, and the azimuth resolution requirement. It was determined that a 0.62 second-per-look integration time meets the 25m resolution requirement. The number of range pulses to be integrated per look is about 1020 at the highest PRF value. An attitude variation of $\pm 1^{\circ}$ in roll, pitch, and yaw corresponds to a doppler frequency range of approximately ± 3000 Hz. Such a doppler frequency range calls for a range walk compensation capability of 128 range bins (complex samples) over the total four-look integration time.

The accuracy required for the doppler frequency and the doppler chirp rate used for azimuth correlation was investigated. A small error in the doppler center frequency causes a slight degradation in the image signal-to-noise ratio. To avoid double features in the processed imagery which result from spectrum foldover, the error must be kept within the difference between the PRF and the processing bandwidth. The doppler chirp rate is a slowly varying function with respect to the target slant range. For single-look high resolution processing, the criterion is that the phase error at both ends of the synthetic aperture, as caused by an incorrect estimate of the chirp rate, must be within $\pm 90^{\circ}$. For multiple-look processing, an error in the chirp rate directly results in misregistration of the pixels produced from single-look processing. To produce 25m resolution 4-look imagery from SEASAT-A SAP, and to limit the misregistration error to within one-quarter of a resolution element, the accuracy of the predicted doppler chirp rate must be within 0.5 Hz per second.

4.2 THE DESIGN OF THE AZIMUTH CORRELATOR

4.2.1 A TIME DOMAIN CORRELATOR ARCHITECTURE

The azimuth correlator performs the correlation between the radar signals and the predicted point target response. The architecture selected must have:

(1) the capability to accommodate the varying doppler characteristics in real-
time, (2) simplicity in the processing control, and (3) amenability to future
on-board implementation. A number of processor architectures are available.
Those using electronic processing techniques include the one-stage and two-
stage fast Fourier transform approaches [5, 6], the time-domain correlation
approaches [7, 8, 9], the digital matched filters [4], etc. For the space-
borne SAR processing application, where high resolution multiple-lock imaging
is required, the time-domain correlation approach was selected for implementa-
tion. Two major advantages associated with the time-domain approach are the
high degree of parallelism that facilitates custom large-scale-integrated (LSI)
circuit implementation, and the relatively simple control for the processing
and multiple-look registration. The selected time-domain architecture, shown
in Figure 4, involves many phase shifters and data accumulators. A more
detailed discussion of this architecture and the associated LSI implementation
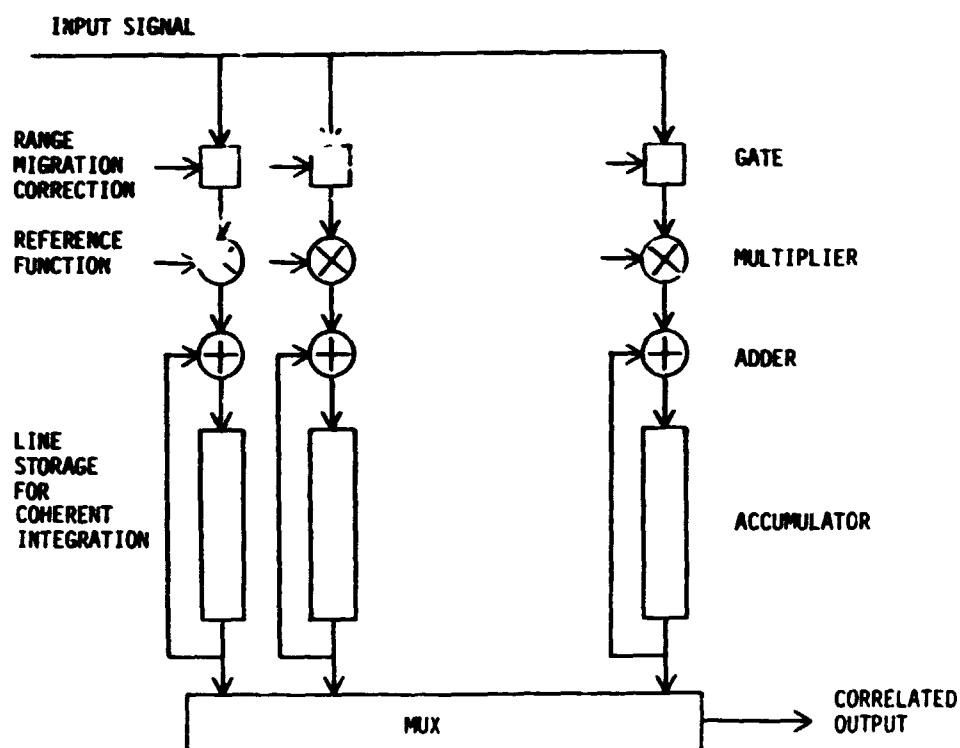consideration is provided in [10].

Fig. 4   A Time-Domain Azimuth Correlator Architecture

4.2.2 MULTIPLE LOOK REGISTRATION

To produce multiple-look imagery, the time-domain correlators are structured
into a number of modules, each producing single look imagery. Assuming that
the doppler center frequency and the doppler chirp rate are known, the phase
reference function over the total synthetic aperture is determined by Eq. 2.
This function will be partitioned into several segments of equal length. Each
segment of the reference function is then used to produce single-look imagery.
This method causes the different looks at each target location to correspond
to data acquired at different times relative to the center of the synthetic
aperture. To overlay the separate looks at the image element, the proper time
delay must be applied to the output of single-look image lines. Using the
right parameters in Eq. 2 for the reference, and assuming that the length of
synthetic aperture is set to be a constant for each look, the timing delay to
register the image lines from adjacent looks is a constant throughout the
swath. (This is much simpler than the multiple-look registration problem
associated with the doppler frequency filtering processing approach. That
approach requires two-dimensional resampling to accomplish accurate registra-
tion of the separate looks at each pixel.)

4.2.3 AZIMUTH CORRELATION WITH PREFILTERING

Each single-look azimuth correlator module is designed to process a portion
of the azimuth bandwidth. The data rate for the correlation processing can
be reduced by implementing prefilters to reduce the data bandwidth. Two kinds
of prefiltering approaches can be used. One approach inserts a bandpass filter
in front of each azimuth correlator. The other approach uses a set of mixers
and lowpass filters to perform the prefiltering.

The time domain correlator architecture shown in Figure 4 can be used to
perform both the prefiltering and the azimuth correlation functions. Reference
function generation is easier to accomplish for the bandpass approach than for
the mixing approach. Using the proposed correlator architecture, the bandpass
filter can be implemented by applying a reference function which is the product
of a finite stage lowpass response and a sinusoidal wave with a frequency equal
to the center frequency of the passband. The reference function for the
azimuth correlator is merely a section of the original phase history of Eq. 2

sampled at a lower rate because of the reduced azimuth bandwidth. Over a wide
swath, the references for both prefiltering and azimuth correlation must be
adjusted to account for the fact that the doppler center frequency and the
doppler chirp rate are dependent on slant range.

The prefiltering approach implemented by mixers has the advantage that ref-
erences for both the front lowpass filtering and the azimuth correlation are
independent of the doppler center frequency. The calculation of the references,
however, is complicated by the fact that variation of the doppler center
frequency along the swath coupled with the target range walk effect introduces
another chirped phase factor into the radar echo signals. To produce high
quality imagery, it would be necessary to compensate for this effect.

The calculation of the reference function has a large effect on the SAR image
quality, therefore, it must be treated very carefully. More detailed descrip-
tion of the reference function and discussions relating to the effects of
phase angle quantization and the number of samples integrated are intended to
be treated in a subsequent paper.

4.2.4 RANGE INTERPOLATION FUNCTION

The input data represent discrete samples of the radar echo signal. The
timing of the sampling pulses is such that they form a rectangular grid in the
two-dimensional range and azimuth plane. However, the range delay history of
a point target follows a near parabolic curve. Therefore, the discrete digital
samples do not coincide with the loci of maximum power return from a point tar-
get. If the processor operated upon the set of discrete samples comprising the
nearest-neighbor approximation of the curved target delay history, it would
cause a loss in the pixel signal-to-noise ratio as well as a broadening of
the target response. Use of range interpolation to introduce points nearer to
the target return curves would perform better than the nearest-neighbor
approach. Both analysis and simulation regarding to the effect of range
interpolation were conducted. Simulation results indicated that a single in-
terpolation which involves the weighted sum of four original range samples and
introduces only one mid point between two samples is as effective as higher
order range interpolation methods. Two fundamental reasons for suggesting

this relatively simple interpolator can be stated as follows: 1) The range spectral response may not be known exactly. 2) The data input for correlation are often quantized to only a few binary bits. These two factors imply that both the interpolation model and the input data will be imperfect. Therefore, the performance of an interpolator will not be a monotonically increasing function of its complexity [11]. Note that interpolation is conducted only along the range direction. The interpolator outputs one interpolated data sample in addition to each original data sample, and it therefore doubles the data rate at the input to the azimuth correlators. The range gates shown in Fig. 4 select the right data sample to be used in subsequent processing.

It has been determined that coherent speckle noise is a major source of distortion on SAR imagery. Error associated with imperfect interpolation is small compared to the speckle noise.

4.3 CORRELATOR DESIGN SUMMARY

Current baseline design of the azimuth correlator uses single-look correlator modules. Each module produces a 20 km swath of 25 m resolution imagery. The time-domain correlator architecture shown in Fig. 4 will be implemented for the single-look modules.

It is also required that the implementation be flexible enough such that a prefiltering operation later can be easily incorporated after real-time processing using the time-domain approach has been demonstrated.

The compatibility between the 20 km correlator module and the overall 100 km swath processing was also considered. Using this 20 km swath correlator as a building block, five modules would be needed for real-time processing of SEASAT-A SAR data. Each module would be associated with its own input and output interface buffers. The data system design incorporating the requirements set forth by the range compression ratio and the synthetic aperture length are summarized in Table 2.

TABLE 2

DATA RATE AND STORAGE DESIGN FOR

REAL-TIME SEASAT-A SAR PROCESSING

Input Interface	
Input Data Rate	45.53 MHz
Width of Input Gating	4096 Samples
Gating Delay Between 20 km Modules	2304 Samples
Double Buffer Data Storage	4096x2 Samples
Output Data Rate	4096xPRF
20 km Correlator Module	
Input Data Rate	4096xPRF
Input Pulse Width	4096 Samples
Range Correlated Pulse Width	1280 Complex
Azimuth Correlator Input Data Rate	1408xPRF
Synthetic Aperture Integration per look	1020 pulses
Range Samples after Azimuth Correlation	1152 Samples
Output Burst Data Rate	1408xPRF
Output Interface	
Input Burst Rate	1408xPRF
Double Buffer Data Storage	1152x2 pixels
Output Data Rate	2.5 MHz

4.4 THE CONTROL PROCESSOR

The main function of the control processor is to derive accurate phase refer-
ences for the synthetic aperture processing. From the previous discussion it
is clear that the doppler center frequency and the doppler frequency rate are
the two major parameters in defining the phase delay history. There are two
ways to determine these two parameters. The first approach which is considered
an exact approach calculates those two parameters based on the relative
position, velocity and acceleration vectors as described in Eq. 1. For an
earth satellite, accurate spacecraft position and velocity vectors may be

derived using the Global Positioning System [12] which is planned to be operational in the 1980 time frame. Once the sensor position is established, the target positions will be determined by a complicated footprint procedure with the antenna attitude as another input. This exact approach appears difficult to perform in real-time because of its complicated arithmetic procedures. For the experimental processor, a simpler approach is proposed which is commonly used on aircraft SAR processing. This approach treats the doppler center frequency and the doppler chirp rate separately. The procedure to determine the doppler center frequency and to generate compensation phase factors is generally referred to as clutterlock.

In spaceborne SAR processing, the uncertainty in the real-time predicts for the antenna attitude may be comparable to the antenna beam width. The purpose of the clutterlock thus is to refine the antenna attitude prediction and thereby maximize the utility of transmitted energy in the azimuth dimension.

For the experimental processor, four-look processing is required. The spectrum selected for processing will be equally partitioned into four parts, each for a single look. It is possible to set the gains of the four single-look correlators to be equal to each other. The image energy of each look thus is proportional to the energy in the corresponding spectral band. The azimuth spectrum will resemble the antenna pattern in that dimension. Let E_i be the energy of the i-th look. A measure which indicates the symmetry of the energy on the looks relative to the center of the processing band can be written as

$$M = (E_1 + E_2 - E_3 - E_4)/(E_1 + E_2 + E_3 + E_4)$$

where the look numbers are ordered as shown in Fig. 5.

By applying proper delay in accumulating the E_j values, it is possible to have the E_i values all correspond to the same target area, therefore the measurement M is independent of any target scene variation. The M value is expected to be zero if a perfect match between the estimated and the true center frequencies is achieved. The integrated value of M can be used to drive a digital version of a voltage controlled oscillator (VCO) to generate a new sinusoidal signal to be mixed with the range correlated signal (to offset the doppler
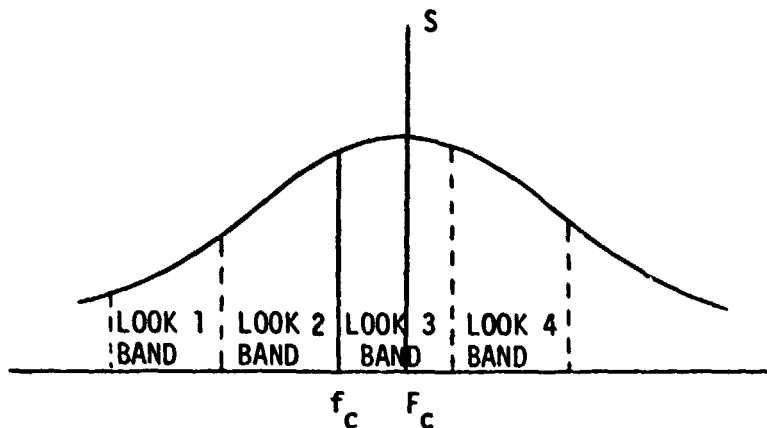
Fig. 5   The Partitioning of a SAR Azimuth
Spectrum for Four-Look Processing

center frequency) or to form a new set of the phase references for azimuth
processing. After this is completed, a new M value will be integrated to the
previously stored M value to generate another offset frequency. The feedback
control in this scheme indeed resembles that of a phase-locked-loop. Since
the M measurement is independent of scene content, convergence can be attained
by properly scaling the integrated M values.

The proposed approach utilizes available single-look image data and it there-
fore minimizes the hardware required to perform this azimuth spectrum anal-
ysis. Preliminary simulation results have indicated that this method can
tolerate a large noise/ambiguity level on the input signals. An example is
briefly discussed here. The original azimuth spectra of four different
signal-to-noise ratios are plotted in Fig. 6. With a processing bandwidth of
approximately 0.8 PRF for a total of four looks, the M values of different
center frequency estimates (normalized to PRF) are plotted in Fig. 7. The
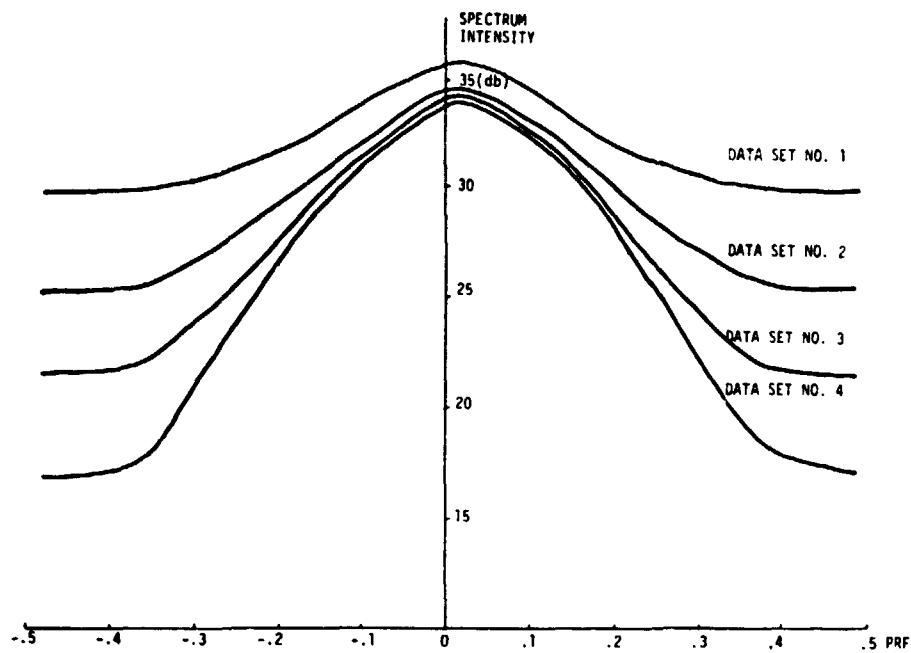position of zero crossings all agree well with the spectral peaks.

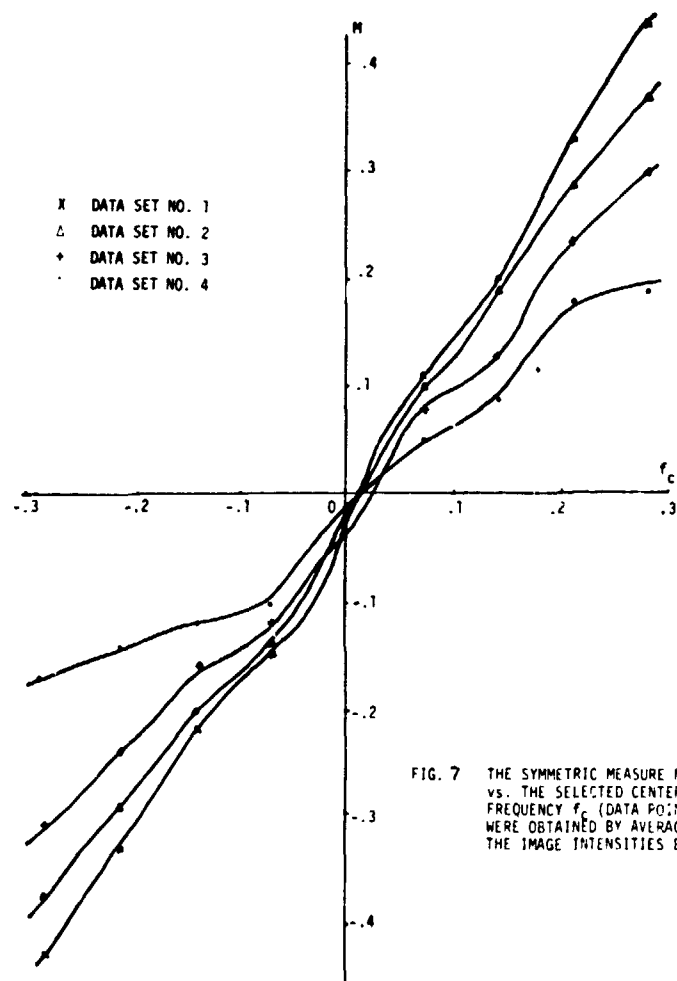FIG. 6   THE FOUR SPECTRAL PATTERNS BEING EVALUATED IN THE SIMULATION.

X   DATA SET NO. 1
△   DATA SET NO. 2
+   DATA SET NO. 3
·   DATA SET NO. 4

FIG. 7   THE SYMMETRIC MEASURE M
vs. THE SELECTED CENTER
FREQUENCY f_c (DATA POINTS
WERE OBTAINED BY AVERAGING
THE IMAGE INTENSITIES E_i).

V-3-17

The clutterlock approach described above measures and reduces the center-band doppler frequency. The remaining parameter, the doppler chirp rate, may be estimated by substituting values of the wavelength, slai. range, relative speed, the gravitational acceleration, and the look angle, into the expression of Eq. 4. Among those quantities, the wavelength is a constant and the slant range for each range sample can be determined from the sample delay. Also, the gravitation and look angle are usually known. The relative speed is a function of both the sensor and target positions. If the space-craft position and velocity are known, the sensor-target relative speed can be estimated using the basic trigonometric operations.

With both the doppler frequency and the frequency rate determined, the phase reference functions to be fed to the azimuth correlator for synthetic aperture processing are well defined. Using the interpulse period as another input, the quadratic phase history is easily obtained by a simple two-step integration of the doppler parameters.

5. CONCLUSION

Real-time processing of spaceborne SAR data is by no means an easy task. Further detailed analysis and simulation are being pursued in an effort to search for better solutions to the SAR processing problem. It is anticipated that this development will serve as a stepping stone toward the implementation of future on-board SAR processors. The utility and practicality of microwave remote sensing from space platforms will be enhanced by the development of high-performance on-board SAR processors.

REFERENCES

[1]   Cutrona, L. J., Synthetic Aperture Radar. Radar Handbook.
       M. I. Skolnik, ed. McGraw-Hill, New York, 1970, Chapter 23.

[2]   Leith, E. N., "Quasi-Holographic Techniques in the Microwave
       Region." IEEE Proc., Vol. 59, No. 9, pp. 1305-1318, Sept. 1971.

[3]   Jordan, R. L., "SEASAT-A Synthetic Aperture Radar Design and
       Implementation." Proceedings of the Synthetic Aperture Radar
       Technology Conference. New Mexico State University, Las Cruces,
       NM, March 1978.

[4]   Wu, C., "A '   al System to Produce Imagery from SAR Data."
       Proceedings   e AIAA System Design Driven by Sensors Con-
       ference, Pap   . 76-968. Pasadena, California, October 1976.

[5]   Kirk, J. C., "A Discussion of Digital Processing for Synthetic
       Aperture Radar," IEEE Trans. on Aerospace and Electronic Sys-
       tems, Vol. AES-11, pp. 326-337, May 1975.

[6]   Martinson, L., "A Programmable Digital Processor for Airborne
       Radar," IEEE 1975 International Radar Conference Record,
       pp. 186-191, April 1975.

[7]   Goodyear Aerospace Corporation, Space Shuttle Synthetic Aper-
       ture Radar-- Final Report, GERA-2113, Submitted to Jet Pro-
       pulsion Laboratory, California Institute of Technology,
       August 1975.

[8]   Arens, W. E., "The Application of Charge-Coupled Device Tech-
       nology to Produce Imagery from Synthetic Aperture Radar Data."
       Proceedings of the AIAA System Design Driven by Sensors Con-
       ference, Paper No. 76-967, Pasadena, California, October 1976.

[9]   Søndergaard, F., "A Dual Mode Digital Processor for Medium Re-
       solution Synthetic Aperture Radar," Paper presented at the
       RADAR-77 Conference, London, October 1977.

[10]   Tyree, V. C., "Custom Large Scale Integrated Circuits for Space-
       Borne SAR Processors," Proceedings of the Synthetic Aperture
       Radar Technology Conference, New Mexico State University, Las
       Cruces, NM, March 1978.

[11]   Allais, D. C., "The Selection of Measurements for Prediction,"
       Technical Report No. 6103-9, Stanford Electronics Laboratories,
       November 1964.

[12]   Smith, D. and Criss, W., "GPS Navstar Global Positioning System,"
       Astronautics and Aeronautics, Vol. 14, No. 4, pp. 26-32, April
       1976.